

# Will the Up and Down Quarks Always Spin Opposite in the Proton?

Tianbo Liu,<sup>1,2,\*</sup> Raza Sabbir Sufian,<sup>1</sup> Guy F. de T ramond,<sup>3</sup>  
Hans G nter Dosch,<sup>4</sup> Stanley J. Brodsky,<sup>5</sup> and Alexandre Deur<sup>1</sup>  
(HLFHS Collaboration)

<sup>1</sup>*Thomas Jefferson National Accelerator Facility, Newport News, VA 23606, USA*

<sup>2</sup>*Department of Physics, Duke University, Durham, NC 27708, USA*

<sup>3</sup>*Laboratorio de F sica Te rica y Computacional, Universidad de Costa Rica, 11501 San Jos , Costa Rica*

<sup>4</sup>*Institut f r Theoretische Physik der Universit t, D-69120 Heidelberg, Germany*

<sup>5</sup>*SLAC National Accelerator Laboratory, Stanford University, Stanford, CA 94309, USA*

We present a new approach motivated by the gauge/gravity correspondence and Veneziano duality to study the spin-dependent quark distributions in the nucleon. The polarized distributions are uniquely determined with no free parameters in terms of the unpolarized ones. The results are consistent with the existing experimental data and agree with the perturbative QCD predictions at large  $x$ . Particularly, we predict the sign change position,  $x \sim 0.8$ , for the down quark polarized distribution, which will be tested very soon in upcoming experiments.

*Introduction.*—Understanding how the spin of the proton originates from its quark and gluon constituents is one of the most active research frontiers in hadron physics [1, 2]. The main task is to determine the polarized parton distribution functions (PDFs),  $\Delta q(x)$ , which describe the difference of the probability density between helicity-parallel and helicity-antiparallel quarks in a proton. Here,  $x$  is the longitudinal momentum fraction carried by quarks of flavor  $q$ . PDFs represent the universal distribution functions of the nucleon. Being determined by the low energy scale characterizing the nucleon size or, equivalently, the confinement scale, they are nonperturbative quantities. It is thus challenging to fully derive them from first principles. However, their  $x$ -dependence at large  $x$  and magnitude in the  $x \rightarrow 1$  limit are predicted by perturbative QCD (pQCD) [3, 4]. This important [3, 5] and rare absolute statement of QCD predicts the helicity retention at  $x \sim 1$ , viz the helicity of a quark carrying large momentum tends to match that of the parent nucleon, which implies that the helicity asymmetry  $\Delta q(x)/q(x)$  approaches 1 as  $x \rightarrow 1$ , with  $q(x)$  being the unpolarized PDF.

During the last decades, precise measurements of  $\Delta q(x)$  became available [1, 2]. While the expected increase of  $\Delta u/u$  toward 1 as  $x \rightarrow 1$  was observed,  $\Delta d/d$  was found to remain negative in the experimentally covered region of  $x \lesssim 0.6$  [6–12], with no indication of a sign change at large  $x$ -value. Global pQCD analyses of the experimental data extrapolated to large  $x$  also favor negative values of  $\Delta d/d$  at  $x \sim 1$  [13–17], as do Dyson-Schwinger equation calculations [18]. This challenges our confidence in understanding the large- $x$  behavior of the polarized PDFs.

In this letter, we present a new approach based on light-front holographic QCD (LFHQCD) [19] and the Veneziano duality [20] to calculate  $\Delta q(x)$ . This offers, for the first time, the possibility of uniquely determining quark polarized distributions from the knowledge of

unpolarized PDFs. Our parameter-free determination of  $\Delta q(x)$  provides an accurate description of the available experimental data and agrees with the pQCD prediction in the  $x \rightarrow 1$  limit. Particularly, the  $x$ -value for the sign change of  $\Delta d/d$  is predicted, which will be tested in upcoming experiments [21, 22].

LFHQCD studies hadron structures by embedding light-front dynamics in a higher dimensional gravity theory [23, 24]. It provides an effective semiclassical approximation to QCD bound state equations [24–27], capturing essential aspects of the strong interaction with the confinement potential determined by the underlying superconformal algebraic structure [28–30]. As a unified framework for the study of spectroscopy and structure, it has been utilized to calculate hadron masses and form factors [19]. With increasing interest in parton distributions, various LFHQCD-based models have been developed, mostly taking the light-front wave functions with some modifications [31–49]. These phenomenological extensions usually require a large number of parameters to accurately describe PDFs, thereby reducing the predictive power. Recently, we introduced a new approach to derive PDFs as well as generalized parton distributions (GPDs) with LFHQCD [50]. It incorporates Regge behaviors at small- $x$  and inclusive counting rules at large- $x$ , and can simultaneously produce the nucleon and pion unpolarized PDFs with minimal parameters, keeping the predictive power with the universality of the reparametrization function. Motivated by such success, we extend here the formalism to polarized distributions, with no additional parameters required.

*Formalism.*—We first briefly review the derivation of unpolarized PDFs from the holographic expression of the spin-non-flip Dirac form factor,  $F_1(t)$ , with  $t = -Q^2$  the square of transferred momentum. The contribution from a twist- $\tau$  state, a component with effectively  $\tau$  constituents, in the Fock expansion of the proton state, to

the Dirac form factor is given by [19, 51]

$$F_1(t) = c_{V,\tau} F_{V,\tau}(t) + c_{V,\tau+1} F_{V,\tau+1}(t), \quad (1)$$

with

$$F_{V,\tau}(t) = \frac{1}{N_{V,\tau}} B\left(\tau - 1, \frac{1}{2} - \frac{t}{4\lambda}\right). \quad (2)$$

The subscript  $V$  indicates the coupling to a vector current.  $\lambda$  is the universal mass scale in LFHQCD, which can be fixed by hadron spectroscopy, and a fitting to the  $\rho/\omega$  trajectory gives  $\sqrt{\lambda} = 0.534 \text{ GeV}$ . The  $c_{V,\tau}$  and  $c_{V,\tau+1}$  are coefficients to be determined,  $N_{V,\tau}$  is a normalization factor, and  $B(x, y)$  is the Euler beta function. The two terms in Eq. (1) correspond to the contribution from two chiral components,  $\Psi_+$  and  $\Psi_-$ , of the bulk field solution [19]. Eq. (2) has the same structure as a generalization of the Veneziano amplitude  $B(1 - \alpha(s), 1 - \alpha(t))$  [20] to non-strong process [52, 53], here electron-nucleon scattering. This amounts to replace the  $s$ -dependence  $1 - \alpha(s)$  by a constant, which determines the asymptotic behaviour of the form factor for large negative values of  $t$  [52, 53]. Our framework thus incorporates nonperturbative analytic structures found in pre-QCD studies, such as Regge trajectories and generalized Veneziano amplitudes.

The  $t$ -dependence in Eq. (2) can be rewritten as  $1 - \alpha_V(t)$  with the Regge trajectory [50]

$$\alpha_V(t) = \frac{t}{4\lambda} + \frac{1}{2}. \quad (3)$$

This is just the  $\rho/\omega$  trajectory emerging from LFHQCD for vector mesons with massless quarks [30]. The quark mass correction is negligible for  $u$  and  $d$  quarks, while for the strange quark contribution one should replace it by the  $\phi$  trajectory, which shifts the intercept to  $\alpha_\phi(0) \approx 0.01$  [54].

The GPDs at zero skewness  $\xi$ , obtained from the integral representation of  $B(x, y)$ , are [50]

$$H_\tau(x, \xi = 0, t) = q_\tau(x) \exp[tf(x)], \quad (4)$$

where the unpolarized PDF  $q_\tau(x)$  and the profile function  $f(x)$  are related by a universal reparameterization function  $w(x)$ ,

$$q_\tau(x) = \frac{1}{N_{V,\tau}} w(x)^{-\frac{1}{2}} [1 - w(x)]^{\tau-2} w'(x), \quad (5)$$

$$f(x) = \frac{1}{4\lambda} \log\left(\frac{1}{w(x)}\right). \quad (6)$$

The function  $w(x)$  obeys the boundary conditions:

$$w(0) = 0, \quad w(1) = 1, \quad w'(x) > 0, \quad (7)$$

$$w'(1) = 0, \quad w''(1) \neq 0. \quad (8)$$

Then for a twist- $\tau$  state, the unpolarized PDF is

$$q(x) = c_{V,\tau} q_\tau(x) + c_{V,\tau+1} q_{\tau+1}(x). \quad (9)$$

Now, we turn to the polarized distributions, for which the coupling of an axial current—rather than a vector current—is needed. Since the current operator only differs by a  $\gamma_5$ , the axial form factor follows Eq. (1) but with a sign flip from the contribution of the chiral-odd component,

$$F_A(t) = c_{A,\tau} F_{A,\tau}(t) - c_{A,\tau+1} F_{A,\tau+1}(t), \quad (10)$$

where

$$F_{A,\tau}(t) = \frac{1}{N_{A,\tau}} B\left(\tau - 1, 1 - \frac{t}{4\lambda}\right), \quad (11)$$

with the subscript  $A$  indicating the coupling to an axial current.  $F_{A,\tau}(t)$  has the same structure as  $F_{V,\tau}(t)$ , but with the Regge trajectory replaced by the axial one:

$$\alpha_A(t) = \frac{t}{4\lambda}, \quad (12)$$

emerging from LFHQCD [30]. The coefficients in (10) and those in (1) are related since they correspond to the same state. Hence, apart from the sign flip in the second term in (10), they should have the same value relative to the normalization factors as given by

$$\frac{c_{V,\tau}}{N_{V,\tau}} = \frac{c_{A,\tau}}{N_{A,\tau}}. \quad (13)$$

Since the normalization convention is arbitrary, we set  $N_{V,\tau} = N_{A,\tau} = N_\tau$ , and therefore identify the coefficients as  $c_{V,\tau} = c_{A,\tau} = c_\tau$  [55].

Following the same procedure, we express the  $\Delta q(x)$  for a twist- $\tau$  state as

$$\Delta q(x) = c_\tau \Delta q_\tau(x) - c_{\tau+1} \Delta q_{\tau+1}(x), \quad (14)$$

where

$$\Delta q_\tau(x) = \frac{1}{N_\tau} [1 - w(x)]^{\tau-2} w'(x). \quad (15)$$

At large- $x$ , we expand  $w(x)$  near  $x = 1$  according to the boundary conditions (7) and (8),

$$w(x) = 1 + \frac{1}{2} w''(1)(1-x)^2 + \mathcal{O}((1-x)^3), \quad (16)$$

and find that  $q_\tau(x)$  and  $\Delta q_\tau(x)$  have the same behavior,

$$q_\tau(x) = \Delta q_\tau(x) = \frac{[-w''(1)]^{\tau-1}}{2^{\tau-2} N_\tau} (1-x)^{2\tau-3} + \dots, \quad (17)$$

where higher powers of  $(1-x)$  are suppressed. For both the  $q(x)$  (9) and the  $\Delta q(x)$  (14), the function is dominated by the first term at large- $x$ , unless its coefficient  $c_\tau = 0$ . Then the helicity asymmetry at  $x \rightarrow 1$  is

$$\lim_{x \rightarrow 1} \frac{\Delta q(x)}{q(x)} = 1, \quad (18)$$

which supports the pQCD prediction [3, 5].

The spin-aligned and spin-antialigned distributions are linear combinations of the unpolarized and polarized distributions written as

$$q_{\uparrow}(x) = \frac{1}{2}[q(x) + \Delta q(x)], \quad (19)$$

$$q_{\downarrow}(x) = \frac{1}{2}[q(x) - \Delta q(x)]. \quad (20)$$

We find, in the large- $x$  limit,

$$q_{\uparrow}(x) \rightarrow c_{\tau} q_{\tau}(x), \quad (21)$$

$$q_{\downarrow}(x) \rightarrow c_{\tau+1} q_{\tau+1}(x). \quad (22)$$

The two helicity distributions tend respectively to a pure contribution from one chiral component,  $\Psi_+$  or  $\Psi_-$ , of the bulk field solution. Eqs. (21) and (22) are referred to as the asymptotic normalization, which can be used to derive the same relation as in Eq. (13).

From Eq. (17),  $q_{\uparrow}(x)$  and  $q_{\downarrow}(x)$  decrease as  $(1-x)^{2\tau-3}$  and  $(1-x)^{2\tau-1}$ , respectively. For the valence state  $\tau = 3$ , they behave as  $(1-x)^3$  and  $(1-x)^5$ , which is consistent with pQCD up to logarithm corrections [3, 4].

At small- $x$ ,  $w(x)$  has a linear  $x$ -dependence:  $w(x) \sim x$ . The  $\Delta q(x)$  decreases faster than the  $q(x)$  with decreasing  $x$ , and the helicity asymmetry behaves as

$$\frac{\Delta q(x)}{q(x)} \sim x^{\frac{1}{2}}, \quad (23)$$

where the exponent  $1/2$  is given by the difference between the intercepts of the vector and axial Regge trajectories (3) and (12), and will be shifted by a negligible amount if  $u$  and  $d$  quarks mass corrections are included. When  $x \rightarrow 0$ , the helicity asymmetry goes to zero,

$$\lim_{x \rightarrow 0} \frac{\Delta q(x)}{q(x)} = 0, \quad (24)$$

which indicates that the helicity correlation between a quark and its parent nucleon disappears. This result is a natural expectation [3], because the constituents and the nucleon have infinite relative rapidity for  $x \sim 0$ . It is confirmed by experimental data [56].

*Numerical results.*—Up to now, all results are derived for arbitrary twist- $\tau$  components without any specific choices for the coefficients  $c_{\tau}$  or for  $w(x)$  as long as the general boundary conditions are fulfilled. For quantitative results of the polarized distributions, the  $c_{\tau}$  values are needed. We determine them via the Dirac form factor. If only valence states are considered, we can express the Dirac form factors of  $u$  and  $d$  quarks as

$$F_1^u(t) = c_{3,u} F_{V,3}(t) + (2 - c_{3,u}) F_{V,4}(t), \quad (25)$$

$$F_1^d(t) = c_{3,d} F_{V,3}(t) + (1 - c_{3,d}) F_{V,4}(t), \quad (26)$$

where the quark number sum rule has been applied with  $N_{\tau} = B(\tau - 1, 1/2)$  normalizing  $F_{V,\tau}(0)$  to 1. Beyond

the valence state of the proton, sea quark constituents are encoded in higher Fock states with additional quark-antiquark pairs. In this work, we truncate the Fock expansion of the nucleon state up to only one quark-antiquark pair, which is a twist-5 state. As a simplifying procedure to include the sea quark contributions we can add to Eq. (25) and Eq. (26) the terms,

$$c_{5,u/d} F_{V,5}(t) - c_{5,u/d} F_{V,6}(t), \quad (27)$$

which assumes that the quark number sum rule is saturated by the contribution from the valence quarks. Furthermore, one can also include the intrinsic strange contribution as in Ref. [54]. We consider the three situations: i) only the valence state contribution; ii) including the contribution from the  $u\bar{u}$  and  $d\bar{d}$  pairs; iii) also including the contribution from the intrinsic strange sea, by taking the results from our previous work [54]. Matching the Dirac form factor with a recent extraction [57], we fix the coefficients, as listed in Table I.

TABLE I. Coefficient values fixed by matching the recent electromagnetic form factor extraction result [57]. The parameter  $a$  in Eq. (31) is fixed by the first moment of unpolarized valence quark distributions for each case. The last column  $g_{A,\min}$  is the isovector axial charge with minimal sea. The meaning of the labels is explained in the text.

Label	$c_{3,u}$	$c_{3,d}$	$c_{5,u}$	$c_{5,d}$	$a$	$g_{A,\min}$
i	1.782	0.066	—	—	0.407	0.867
ii	1.793	0.062	-0.559	-0.516	0.480	0.879
iii	1.794	0.060	-0.492	-0.447	0.471	0.881

Since electromagnetic form factors only measure the difference between quark and antiquark contributions, namely  $c_{\tau,u} \equiv u_{\tau} - \bar{u}_{\tau}$  and similarly for the  $d$  quark, adding equal terms to  $u_{\tau}$  and  $\bar{u}_{\tau}$  does not modify the form factor, they cannot be uniquely separated. However, a lower boundary can be derived from the positivity bounds  $q_{\uparrow}(x) \geq 0$  and  $q_{\downarrow}(x) \geq 0$ . With the asymptotic relations (21) and (22), this requirement is fulfilled by the minimal sea contribution,

$$\bar{u}(x)_{\min} = c_{5,u} q_{\tau=6}(x) \quad \text{if } c_{5,u} \geq 0, \quad (28)$$

$$\bar{u}(x)_{\min} = -c_{5,u} q_{\tau=5}(x) \quad \text{if } c_{5,u} < 0, \quad (29)$$

and similarly for  $\bar{d}$ . This constraint is stronger than that utilized in Ref. [54], where only the sum  $q_{\uparrow}(x) + q_{\downarrow}(x) \geq 0$  is required.

Since the sea quark distributions are not separately constrained by electromagnetic form factors, one needs other physical observables that are sensitive to the quark and antiquark contributions individually to determine them separately. Instead of attempting a full separation, which is beyond the purpose of this work, we use the axial sum rule,

$$g_A = (\Delta u + \Delta \bar{u}) - (\Delta d + \Delta \bar{d}), \quad (30)$$

to constrain the non-minimal sea quark.

The value of the isovector axial charge  $g_A = 1.2732(23)$  is precisely determined by the neutron weak decay [58]. As shown in Table I, its values evaluated with a minimal sea component,  $g_{A,\min}$ , are smaller than the experimental value. To in the value of  $g_A$  with the minimal shift  $u_\tau \rightarrow u_\tau + \delta_{\tau,u}$ ,  $\bar{u}_\tau \rightarrow \bar{u}_\tau + \delta_{\tau,u}$  and similarly for the  $d$ -quark, implies a positive shift  $\delta_{\tau=5,u}$  and/or  $\delta_{\tau=6,d}$ . Therefore, we satisfy the sum rule by the shift  $\delta_{\tau=5,u}$  and  $\delta_{\tau=6,d}$ , and take the variation between them as part of the theoretical uncertainty.

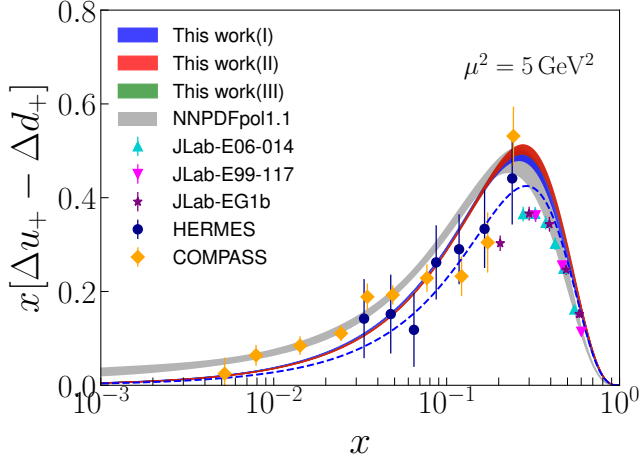


FIG. 1. Polarized distributions of the isovector combination  $x[\Delta u_+(x) - \Delta d_+(x)]$  in comparison with NNPDF global fit [15] and experimental data [6–10, 12]. Three sets of parameters, see Table I, are determined from the Dirac form factor and unpolarized valence distributions. The bands represent the variation with different approaches to saturate the axial sum rule. The blue dashed curve shows the result with only valence state contribution.

For the universal reparametrization function  $w(x)$ , we take the same form as in [50],

$$w(x) = x^{1-x} \exp[-a(1-x)^2], \quad (31)$$

with the parameter “ $a$ ” fixed with the first moment of unpolarized valence quark distributions. One can in principle adopt any parametrization form that fulfills the boundary conditions (7) and (8), and the predictive power is kept by the universality of  $w(x)$  for all PDFs. For comparison with measurements, we evolve the distributions from 1.06 GeV, which is the matching scale suggested by the study of the strong coupling constant [59]. As shown in Figs. 1-3, our numerical results are in good agreement with the global fit [15] and measurements [6–10, 12]. The isovector combination  $\Delta u_+ - \Delta d_+$ , where  $u_+$  and  $d_+$  stand for  $u + \bar{u}$  and  $d + \bar{d}$ , is the distribution relevant to the axial charge sum rule (30). In Fig. 1, the dashed blue curve is the contribution from the valence state only, and the difference with the full results,

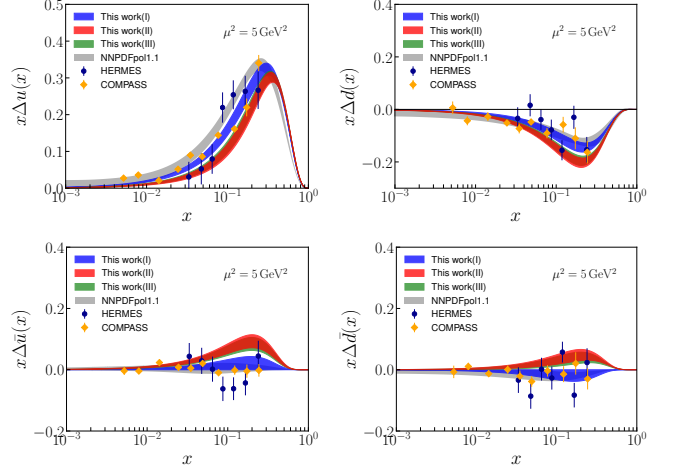


FIG. 2. Polarized distributions of  $u$ ,  $d$ ,  $\bar{u}$ , and  $\bar{d}$  in comparison with NNPDF global fit [15] and experimental data [10, 12]. The bands have the same meaning as in Fig. 1.

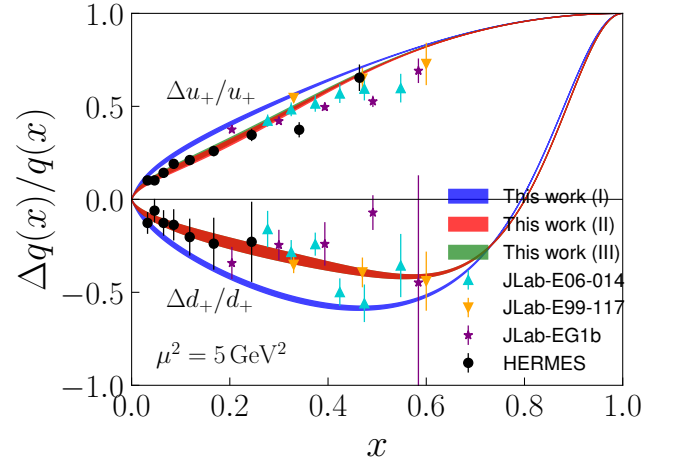


FIG. 3. Helicity asymmetries of  $u + \bar{u}$  and  $d + \bar{d}$  compared with measurements. The bands and symbols have the same meaning as in Fig. 1.

cases I, II and III, which include saturation of the axial sum rule is noticeable. This is consistent with the analysis of the Pauli form factor in [60], which demonstrates the significance of the sea quarks in describing spin-related quantities. For each single flavor, shown in Fig. 2, the variation of the results with three sets of coefficients is large, because the sea quark coefficients are not well constrained by the procedure discussed above. Furthermore, the truncation of the Fock state up to five-quark states allowing only one pair of sea quarks may potentially result in greater theoretical uncertainties for each individual flavor. The axial sum rule provides an important constraint but still leave some flexibility, like adding the same term to  $u\bar{u}$  and  $d\bar{d}$ . Since the goal of this letter is to introduce a new approach to study polarized



PDFs, we leave this issue to future more detailed investigations. Importantly, the critical region for the upcoming Jefferson Lab spin program [21, 22] is the large- $x$  region, which is dominated by the valence state and is thus much less affected by the variation of the sea. As observed in Fig. 3, the results with three sets of coefficients are quite consistent in the large- $x$  region. As we have analytically demonstrated above, our approach supports the pQCD prediction that the helicity asymmetry approaches 1 at large- $x$  limit and follows the power behavior  $(1-x)^2$ . In particular, the  $d$ -quark helicity change is robustly predicted around  $x \sim 0.8$ .

*Summary.*—We present a new approach to study the spin-dependent quark distributions. Our analytic result is consistent with the pQCD large- $x$  behavior. It also supports the pQCD prediction of the helicity retention at  $x \sim 1$ , which is not indicated by existing data and is challenged by Dyson-Schwinger equation calculations, particularly for the  $d$ -quark. With all parameters fixed by the nucleon Dirac form factor and unpolarized quark distributions, our results of polarized distributions agree with existing data. In the large- $x$  region, where the valence state dominates, we find the  $d$ -quark helicity flips its sign around  $x \sim 0.8$ , regardless of the procedure used to include the sea quark contribution. This prediction will be tested soon [21, 22]. The analytic behavior at large- $x$  and the agreement with existing data consolidates our confidence in the pQCD prediction, which can be implemented in global analysis such as in Ref. [61]. In addition, the relation between the unpolarized and polarized distributions also sheds light on a possible simultaneous global fit of unpolarized and polarized PDFs.

We would like to thank J.-P. Chen for helpful discussions. This work is supported in part by the U.S. Department of Energy, Office of Science, Office of Nuclear Physics under contracts No. DE-AC05-06OR23177 and No. DE-FG02-03ER41231.

---

\* liutb@jlab.org

- [1] A. Deur, S. J. Brodsky, and G. F. de Téramond, The Spin Structure of the Nucleon, *Rep. Prog. Phys.* **82**, 076201 (2019).
- [2] C. A. Aidala, S. D. Bass, D. Hasch, and G. K. Mallot, The Spin Structure of the Nucleon, *Rev. Mod. Phys.* **85**, 655 (2013).
- [3] S. J. Brodsky, M. Burkardt, and I. Schmidt, Perturbative QCD constraints on the shape of polarized quark and gluon distributions, *Nucl. Phys. B* **441**, 197 (1995).
- [4] H. Avakian, S. J. Brodsky, A. Deur, and F. Yuan, Effect of Orbital Angular Momentum on Valence-Quark Helicity Distributions, *Phys. Rev. Lett.* **99**, 082001 (2007).
- [5] G. R. Farrar and D. R. Jackson, Pion and Nucleon Structure Functions Near  $x = 1$ , *Phys. Rev. Lett.* **35**, 1416 (1975).
- [6] X. Zheng *et al.* (Jefferson Lab Hall A Collaboration), Precision measurement of the neutron spin asymmetry  $A_1^N$  and spin flavor decomposition in the valence quark region, *Phys. Rev. Lett.* **92**, 012004 (2004).
- [7] X. Zheng *et al.* (Jefferson Lab Hall A Collaboration), Precision measurement of the neutron spin asymmetries and spin-dependent structure functions in the valence quark region, *Phys. Rev. C* **70**, 065207 (2004).
- [8] D. S. Parno *et al.* (Jefferson Lab Hall A Collaboration), Precision Measurements of  $A_1^n$  in the Deep Inelastic Regime, *Phys. Lett. B* **744**, 309 (2015).
- [9] K. V. Dharmawardane *et al.* (CLAS Collaboration), Measurement of the  $x$ - and  $Q^2$ -dependence of the asymmetry  $A_1$  on the nucleon, *Phys. Lett. B* **641**, 11 (2006).
- [10] A. Airapetian *et al.* (HERMES Collaboration), Flavor decomposition of the sea-quark helicity distributions in the nucleon from semiinclusive deep inelastic scattering, *Phys. Rev. Lett.* **92**, 012005 (2004).
- [11] A. Airapetian *et al.* (HERMES Collaboration), Quark helicity distributions in the nucleon for up, down, and strange quarks from semi-inclusive deep-inelastic scattering, *Phys. Rev. D* **71**, 012003 (2005).
- [12] M. G. Alekseev *et al.* (COMPASS Collaboration), Quark helicity distributions from longitudinal spin asymmetries in muon-proton and muon-deuteron scattering, *Phys. Lett. B* **693**, 227 (2010).
- [13] D. de Florian, R. Sassot, M. Stratmann, and W. Vogelsang, Global Analysis of Helicity Parton Densities and Their Uncertainties, *Phys. Rev. Lett.* **101**, 072001 (2008).
- [14] D. de Florian, R. Sassot, M. Stratmann, and W. Vogelsang, Extraction of Spin-Dependent Parton Densities and Their Uncertainties, *Phys. Rev. D* **80**, 034030 (2009).
- [15] E. R. Nocera, R. D. Ball, S. Forte, G. Ridolfi, and J. Rojo, A first unbiased global determination of polarized PDFs and their uncertainties, *Nucl. Phys. B* **887**, 276 (2014).
- [16] P. Jimenez-Delgado, H. Avakian, and W. Melnitchouk, Constraints on spin-dependent parton distributions at large  $x$  from global QCD analysis, *Phys. Lett. B* **738**, 263 (2014).
- [17] J. J. Ethier, N. Sato, and W. Melnitchouk, First simultaneous extraction of spin-dependent parton distributions and fragmentation functions from a global QCD analysis, *Phys. Rev. Lett.* **119**, no. 13, 132001 (2017).
- [18] C. D. Roberts, R. J. Holt and S. M. Schmidt, Nucleon spin structure at very high- $x$ , *Phys. Lett. B* **727**, 249 (2013).
- [19] For a review, see *e.g.*, S. J. Brodsky, G. F. de Téramond, H. G. Dosch and J. Erlich, Light-front holographic QCD and emerging confinement, *Phys. Rep.* **584**, 1 (2015).
- [20] G. Veneziano, Construction of a crossing - symmetric, Regge behaved amplitude for linearly rising trajectories, *Nuovo Cim. A* **57**, 190 (1968).
- [21] JLab experiment E12-06-110, spokespersons: X. Zheng (contact), G. Cates, J.-P. Chen, and Z.-E. Meziani.
- [22] JLab experiment E12-06-122, spokespersons: B. Wojtsekhowski (contact), J. Annand, T. Averett, G. Cates, N. Liyanage, G. Rosner, and X. Zheng.
- [23] S. J. Brodsky and G. F. de Téramond, Light-front hadron dynamics and AdS/CFT correspondence, *Phys. Lett. B* **582**, 211 (2004).
- [24] S. J. Brodsky, G. F. de Téramond, and H. G. Dosch, Threefold Complementary Approach to Holographic QCD, *Phys. Lett. B* **729**, 3 (2014).

- [25] G. F. de Téramond and S. J. Brodsky, Hadronic spectrum of a holographic dual of QCD, *Phys. Rev. Lett.* **94**, 201601 (2005).
- [26] S. J. Brodsky and G. F. de Téramond, Hadronic spectra and light-front wavefunctions in holographic QCD, *Phys. Rev. Lett.* **96**, 201601 (2006).
- [27] G. F. de Téramond and S. J. Brodsky, Light-Front Holography: A First Approximation to QCD, *Phys. Rev. Lett.* **102**, 081601 (2009).
- [28] G. F. de Téramond, H. G. Dosch, and S. J. Brodsky, Baryon Spectrum from Superconformal Quantum Mechanics and its Light-Front Holographic Embedding, *Phys. Rev. D* **91**, no. 4, 045040 (2015).
- [29] H. G. Dosch, G. F. de Téramond, and S. J. Brodsky, Superconformal Baryon-Meson Symmetry and Light-Front Holographic QCD, *Phys. Rev. D* **91**, no. 8, 085016 (2015).
- [30] S. J. Brodsky, G. F. de Téramond, H. G. Dosch, and C. Lorcé, Universal Effective Hadron Dynamics from Superconformal Algebra, *Phys. Lett. B* **759**, 171 (2016).
- [31] Z. Abidin and C. E. Carlson, Hadronic Momentum Densities in the Transverse Plane, *Phys. Rev. D* **78**, 071502 (2008).
- [32] A. Vega, I. Schmidt, T. Gutsche, and V. E. Lyubovitskij, Generalized parton distributions in AdS/QCD, *Phys. Rev. D* **83**, 036001 (2011).
- [33] A. Vega, I. Schmidt, T. Gutsche, and V. E. Lyubovitskij, Generalized parton distributions in an AdS/QCD hard-wall model, *Phys. Rev. D* **85**, 096004 (2012).
- [34] T. Gutsche, V. E. Lyubovitskij, I. Schmidt, and A. Vega, Light-front quark model consistent with Drell-Yan-West duality and quark counting rules, *Phys. Rev. D* **89**, no. 5, 054033 (2014) [Erratum: *Phys. Rev. D* **92**, no. 1, 019902 (2015)].
- [35] T. Gutsche, V. E. Lyubovitskij, I. Schmidt, and A. Vega, Nucleon structure in a light-front quark model consistent with quark counting rules and data, *Phys. Rev. D* **91**, 054028 (2015).
- [36] D. Chakrabarti and C. Mondal, Generalized Parton Distributions for the Proton in AdS/QCD, *Phys. Rev. D* **88**, no. 7, 073006 (2013).
- [37] D. Chakrabarti and C. Mondal, Chiral-odd generalized parton distributions for proton in a light-front quark-diquark model, *Phys. Rev. D* **92**, no. 7, 074012 (2015).
- [38] M. Dehghani, Hard-gluon Evolution of Nucleon Generalized Parton Distributions in Soft-Wall AdS/QCD Model, *Phys. Rev. D* **91**, no. 7, 076009 (2015).
- [39] D. Chakrabarti, T. Maji, C. Mondal, and A. Mukherjee, Quark Wigner distributions and spin-spin correlations, *Phys. Rev. D* **95**, no. 7, 074028 (2017).
- [40] C. Mondal, N. Kumar, H. Dahiya, and D. Chakrabarti, Charge and longitudinal momentum distributions in transverse coordinate space, *Phys. Rev. D* **94**, no. 7, 074028 (2016).
- [41] T. Maji and D. Chakrabarti, Light front quark-diquark model for the nucleons, *Phys. Rev. D* **94**, no. 9, 094020 (2016).
- [42] T. Maji and D. Chakrabarti, Transverse structure of a proton in a light-front quark-diquark model, *Phys. Rev. D* **95**, no. 7, 074009 (2017).
- [43] M. Traini, M. Rinaldi, S. Scopetta, and V. Vento, The effective cross section for double parton scattering within a holographic AdS/QCD approach, *Phys. Lett. B* **768**, 270 (2017).
- [44] T. Gutsche, V. E. Lyubovitskij, and I. Schmidt, Nucleon parton distributions in a light-front quark model, *Eur. Phys. J. C* **77**, no. 2, 86 (2017).
- [45] T. Maji, C. Mondal, and D. Chakrabarti, Leading twist generalized parton distributions and spin densities in a proton, *Phys. Rev. D* **96**, no. 1, 013006 (2017).
- [46] M. Rinaldi, GPDs at non-zero skewness in ADS/QCD model, *Phys. Lett. B* **771**, 563 (2017).
- [47] A. Bacchetta, S. Cotogno, and B. Pasquini, The transverse structure of the pion in momentum space inspired by the AdS/QCD correspondence, *Phys. Lett. B* **771**, 546 (2017).
- [48] C. Mondal, Helicity-dependent generalized parton distributions for nonzero skewness, *Eur. Phys. J. C* **77**, no. 9, 640 (2017).
- [49] N. Chouika, C. Mezrag, H. Moutarde, and J. Rodríguez-Quintero, Covariant Extension of the GPD overlap representation at low Fock states, *Eur. Phys. J. C* **77**, no. 12, 906 (2017).
- [50] G. F. de Téramond, T. Liu, R. S. Sufian, H. G. Dosch, S. J. Brodsky, and A. Deur, Universality of Generalized Parton Distributions in Light-Front Holographic QCD, *Phys. Rev. Lett.* **120**, no. 18, 182001 (2018).
- [51] S. J. Brodsky and G. F. de Téramond, AdS/CFT and Light-Front QCD, *Subnucl. Ser.* **45**, 139 (2009).
- [52] M. Ademollo and E. Del Giudice, Nonstrong amplitudes in a Veneziano-type model, *Nuovo Cim. A* **63**, 639 (1969).
- [53] P. V. Landshoff and J. C. Polkinghorne, The scaling law for deep inelastic scattering in a new veneziano-like amplitude, *Nucl. Phys. B* **19**, 432 (1970).
- [54] R. S. Sufian, T. Liu, G. F. de Téramond, H. G. Dosch, S. J. Brodsky, A. Deur, M. T. Islam, and B.-Q. Ma, Nonperturbative strange-quark sea from lattice QCD, light-front holography, and meson-baryon fluctuation models, *Phys. Rev. D* **98**, no. 11, 114004 (2018).
- [55] The normalization convention used here corresponds to  $\int_0^1 dx q_T(x) = 1$ , and  $\int_0^1 dx \Delta q_T(x) = \frac{\Gamma(\tau-1/2)}{\sqrt{\pi}\Gamma(\tau)}$ .
- [56] E. R. Nocera, Small- and large- $x$  nucleon spin structure from a global QCD analysis of polarized Parton Distribution Functions, *Phys. Lett. B* **742**, 117 (2015).
- [57] Z. Ye, J. Arrington, R. J. Hill, and G. Lee, Proton and Neutron Electromagnetic Form Factors and Uncertainties, *Phys. Lett. B* **777**, 8 (2018).
- [58] M. Tanabashi *et al.* (Particle Data Group), Review of Particle Physics, *Phys. Rev. D* **98**, no. 3, 030001 (2018).
- [59] A. Deur, S. J. Brodsky and G. F. de Téramond, Determination of  $\Lambda_{\overline{\text{MS}}}$  at five loops from holographic QCD, *J. Phys. G* **44**, no. 10, 105005 (2017).
- [60] R. S. Sufian, G. F. de Téramond, S. J. Brodsky, A. Deur, and H. G. Dosch, Analysis of nucleon electromagnetic form factors from light-front holographic QCD : The spacelike region, *Phys. Rev. D* **95**, no. 1, 014011 (2017).
- [61] E. Leader, A. V. Sidorov, and D. B. Stamenov, A New evaluation of polarized parton densities in the nucleon, *Eur. Phys. J. C* **23**, 479 (2002).